Hindawi
Shock and Vibration
Volume 2021, Article ID 5272878, 10 pages
https://doi.org/10.1155/2021/5272878

Research Article

Study on Dynamic Evolution Law of Blasting Cracks in Elliptical Bipolar Linear Shaped Charge Blasting

Bo Wu,[1,2,3] **Shixiang Xu**,[1,4] **Guowang Meng**,[1,4] **Junhua Cai**,[5] **Han Wei**,[1,4] **Hualong Li**,[1,4] **and Jinglong Zhang**[1,4]

[1]*College of Civil Engineering and Architecture, Guangxi University, Nanning, Guangxi 530004, China*
[2]*School of Civil and Architectural Engineering, East China University of Technology, Nanchang, Jiangxi 330013, China*
[3]*School of Architectural Engineering, Guangzhou City Construction College, Guangzhou, Guangdong 510925, China*
[4]*The Key Laboratory of Disaster Prevention and Structural Safety of Ministry of Education, Guangxi University, Nanning, Guangxi 530004, China*
[5]*Sanming Puyan Expressway Co. Ltd., Sanming, Fujian 365000, China*

Correspondence should be addressed to Shixiang Xu; 603559081@qq.com

Received 13 April 2021; Revised 21 May 2021; Accepted 11 June 2021; Published 28 June 2021

Academic Editor: Bangbiao Wu

Based on LS-DYNA numerical simulation analysis and comparison with laboratory tests, the blasting crack development dynamic evolution mechanism of elliptical bipolar linear shaped charge is analyzed. The development law of rock crack and optimal radial decoupling coefficient under different blast hole diameters were studied. The results revealed that the blasting with elliptical bipolar linear shaped charge had a remarkable effect on the directional crack formation, and the maximum effective stress of rock close to the position of shaped charge in the direction of concentrating energy is about 2.3 times of that in the direction of nonconcentrated energy. Moreover, the directional crack could be formed by blasting with elliptical bipolar linear shaped charge with different hole diameters, whilst the length of the main crack was related to the radial decoupling coefficient. Particularly, the main crack reached the longest when the radial decoupling coefficient was 3.36.

1. Introduction

China has become the country with the largest scale, the largest number, and the highest difficulty of tunnel construction in the world [1]. According to statistics, by the end of 2020, China's railway operating mileage had reached 145000 km, of which 16798 railway tunnels had been put into operation, with a total length of about 19630 km [2]. In addition to the tunnel boring machine, the drilling and blasting method is still widely utilized in rock tunnel construction. Improper control of traditional drilling and blasting methods would easily lead to engineering and social problems such as vibration hazard, environmental pollution, instability of surrounding rock, and serious overbreak and underbreak, which seriously restrict the construction process of tunnel engineering [3].

In order to solve the above problems, directional fracture controlled blasting technology is often used at present. Many scholars have conducted in-depth research around the rock failure mechanism and directional fracture effect of directional fracture controlled blasting. For instance, Cho et al. [4] combined model test and numerical simulation method to study the influence of empty hole on crack propagation under different blasting and comprehensively analyzed the relationship between fracture energy and crack propagation. Yang et al. [5–8] adopted a testing system of digital laser dynamic caustics to study the influence of different cutting angle, depth, initial stress field, and other factors on the crack propagation of slotted cartridge blasting and then analyzed the mechanism of crack extension and penetration. Yue et al. [9–12] used a new testing system of digital laser dynamic caustics to carry out the experimental research on the

development of blasting crack under slotted cartridge blasting, whilst obtained the crack extension velocity, acceleration, dynamic stress intensity factor at the front end of the crack, and the law of dynamic energy release rate. Wang [13] explored the formation of detonation and initial crack of slotted cartridge blasting and the relationship between decoupling coefficient and blasting damage based on numerical simulation. Luo et al. [14, 15] made a preliminary study on the formation of guided crack, crack initiation, propagation, and penetration of shaped charge. In 2006, the Sinohydro Engineering Bureau 8 Co., Ltd. developed an elliptical bipolar linear shaped charge (EBLSC), which performed well in practical engineering applications [16]. Li et al. [17, 18] further conducted theoretical analysis, numerical simulation, and experimental research on the blasting of EBLSC, and the research showed that this charge structure has a good application effect and prospect in presplit blasting. Subsequently, the elliptical bipolar linear shaped charge blasting technology has been widely promoted and applied in engineering. Wu et al. [19–21] carried out a preliminary study on the blasting mechanism, influencing factors, and crack development of elliptical bipolar linear shaped charge blasting.

However, for the directional controlled blasting technology, most of the research studies are focused on the slotted cartridge blasting, while the research on the evolution law of shaped charge blasting crack is less. The rock breaking mechanism of elliptical bipolar shaped charge blasting excavation is not clear. In this paper, the rock failure mechanism, the temporal and spatial law of crack development, and decoupling coefficient of elliptical bipolar linear shaped charge blasting were studied. Moreover, the optimal decoupling coefficient was obtained via analyzing the crack development law of different blast hole diameters, which provide an important reference for practical engineering application.

2. Analysis of the Rock Failure Mechanism of Shaped Charge Blasting

The detonation products of conventional blasting scattered irregularly around the blast hole, and the cracks also expanded irregularly [22]. The shaped charge blasting uses a layer liner to change the structure of the explosive to make the detonation products accumulate in a specific direction and improve the destructive effect in a specific direction [23].

An energy cavity is set at the symmetrical position on both sides of the shaped charge. The detonation products generated by blasting will accumulate along the axis of the energy cavity to form a high-density, high-speed, and high-pressure air flow, which is called shaped charge jet [24]. The shaped charge jet penetrates the rock and produces the initial guide crack, which provides a directional effect for the subsequent explosion stress wave and blasting gas to further expand the crack. According to the rock fracture mechanics, a dynamic fracture mechanics model of shaped charge blasting is established, as shown in Figure 1.

During crack propagation, the stress intensity factor at the crack tip is as follows [25]:

$$K_1 = PF\sqrt{\pi\left(r_b + a\right)} + \sigma_\theta\sqrt{\pi a}. \quad (1)$$

Thereinto, P is the explosive gas pressure in the fracture; F is the correction factor of stress intensity factor; r_b is the blast hole radius; a is the fracture length; and σ_θ is the tangential stress.

According to the theory of fracture mechanics, $K_1 > K_{IC}$, the crack initiates and propagates, where K_{IC} represents the fracture toughness of the rock. Therefore, to ensure that the crack continues to grow, the pressure of detonation gas should meet the following conditions:

$$P > \frac{K_{IC} - \sigma_\theta\sqrt{\pi a}}{F\sqrt{\pi\left(r_b + a\right)}}. \quad (2)$$

The guiding crack penetrated by the shaped energy jet is much larger than the other small cracks in the crushing zone. After blasting, a large amount of high-pressure explosive gas will be introduced, and the pressure of the explosive gas in the concentrating energy direction will increase; that is, the P will increase; according to the law of conservation of energy, the effect of explosive gas in the nonconcentrated energy direction will be weakened, and the P will decrease. Therefore, while the structure of the shaped charge leads to an increase in the evolution ability of cracks in the direction of concentrating energy, it also reduces the ability of evolution of cracks in the direction of nonconcentrated energy.

3. Validation of Numerical Solution

3.1. Explosion Test of PMMA. Polymethyl methacrylate (PMMA) is usually used as an ideal test material to study the crack propagation process of PMMA under laboratory conditions. Its main advantage is transparency, which makes the crack morphology easy to be observed directly by naked eyes. The fracture mechanical behavior of this material is similar to that of brittle rock [26, 27]. The test results of Rossmanith et al. [28] also suggested that the blasting cracks could be divided into the following three areas: crushing zone, radial microcrack zone, and radial crack zone. The crack morphology of PMMA is very similar to that of rock under dynamic loading. Hence, it can be considered that the blasting test results of PMMA are consistent with those of rock materials, which is suitable for exploring the mechanism of crack initiation and propagation near the blast hole and in the far-field area.

Che [29] carried out the blasting test of a shaped charge with PMMA, wherein the outer diameter of the shaped charge was 7 mm, the inner diameter was 5 mm, the energy gathering tube was made of PVC material, and the thickness of the shell of the energy gathering tube was 1 mm. The structure design of the shaped charge is shown in Figure 2. The geometric size of the specimen was 300 mm × 200 mm × 100 mm. The blast hole was located in the center of the specimen, and the diameter of the blast hole was 12 mm. The specimen of PMMA is shown in Figure 3. The crack development was recorded by the digital laser dynamic caustics test system.

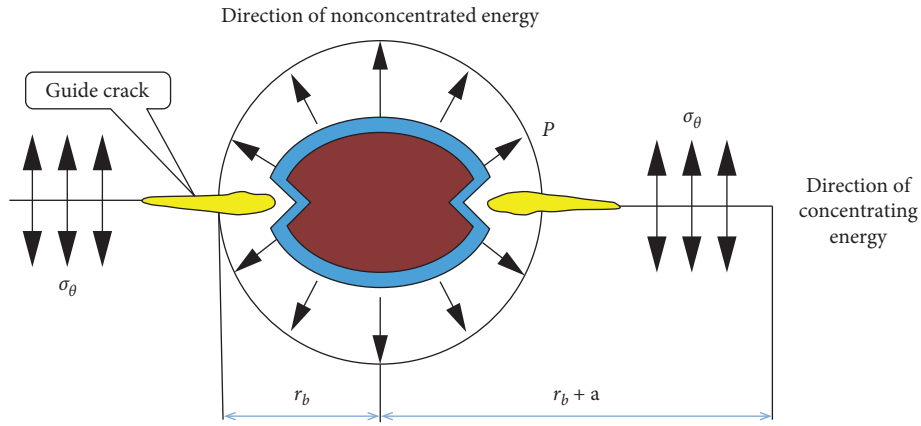

Figure 1: Mechanical model of cracking due to shaped charge blasting.

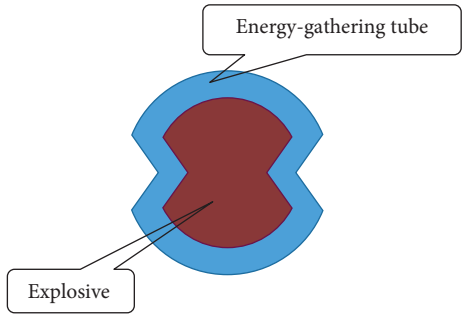

Figure 2: Structure design of shaped charge [29].

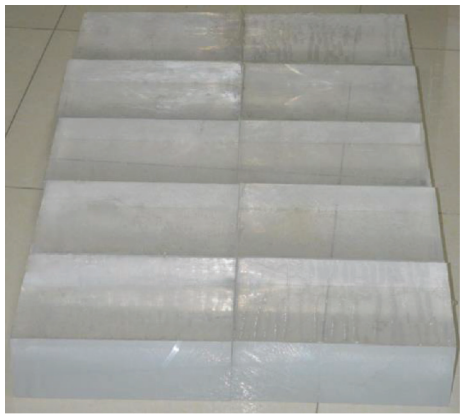

Figure 3: The specimen of PMMA [29].

The test results are shown in Figure 4. Next, numerical simulation analysis would be carried out for the blasting test to verify the effectiveness of the finite element solution.

3.2. Numerical Model. Using LS-DYNA nonlinear dynamic analysis software to carry out numerical simulation analysis, the geometric size of the model is the same as the above model test. A nonreflective boundary condition is added to simulate an infinite plane to eliminate the interference of reflected waves at the boundary. In the numerical model, the material model of the explosive is characterized by MAT_HIGH_EXPLOSIVE_BURN, and the relationship between the pressure and volume of the explosive after detonation is described by the JWL state equation.

$$p = A\left(1 - \frac{\omega}{R_1 V}\right)^{-R_1 V} + B\left(1 - \frac{\omega}{R_2 V}\right) + \frac{\omega E}{V}, \quad (3)$$

where p is the pressure, V is the volume, A, B, ω, R_1, and R_2 are the basic parameters of the equation of state, and E is the initial internal energy per unit volume. Explosive and state equation parameters are shown in Table 1.

The PVC energy gathering tube material adopts the model MAT_PLASTIC_KINEMATIC, and the mechanical parameter of the PVC is shown in Table 2.

The MAT_NULL model and the EOS_LINEAR_POLYNOMIAL state equation are used to simulate air, the HJC constitutive model is used for rock, and the failure mode is added to analyze crack development. The main rock parameter is shown in Table 3.

3.3. Analysis of Numerical Simulation Results. Figure 5 shows the development of blasting cracks at different times. The blasting cavity is formed after 20 μs of detonation, and the length of the cracks in the concentrating energy direction is significantly greater than the length of the cracks in other directions. At 80 μs, microcracks appear in other directions, and the crack in the concentrating energy direction keeps growing. At 120 μs, the crack in the direction of energy accumulation and other directions keeps growing. At 600 μs, the crack tends to stop and the crack in the concentrating energy direction is always larger than that of the other directions.

Compared with Figure 4, the results in Figure 5 indicate that the numerical simulation completely reproduces the crushing zone around the hole, the crack initiation, and development process in the concentrating energy direction and other directions of the PMMA under the shaped charge blasting. The final distribution of blasting cracks is in good agreement with the experimental results, thus proving the correctness of the established model and its numerical solution. Next, the numerical model will be used to study the evolution law of blasting cracks in elliptical bipolar linear shaped charge blasting.

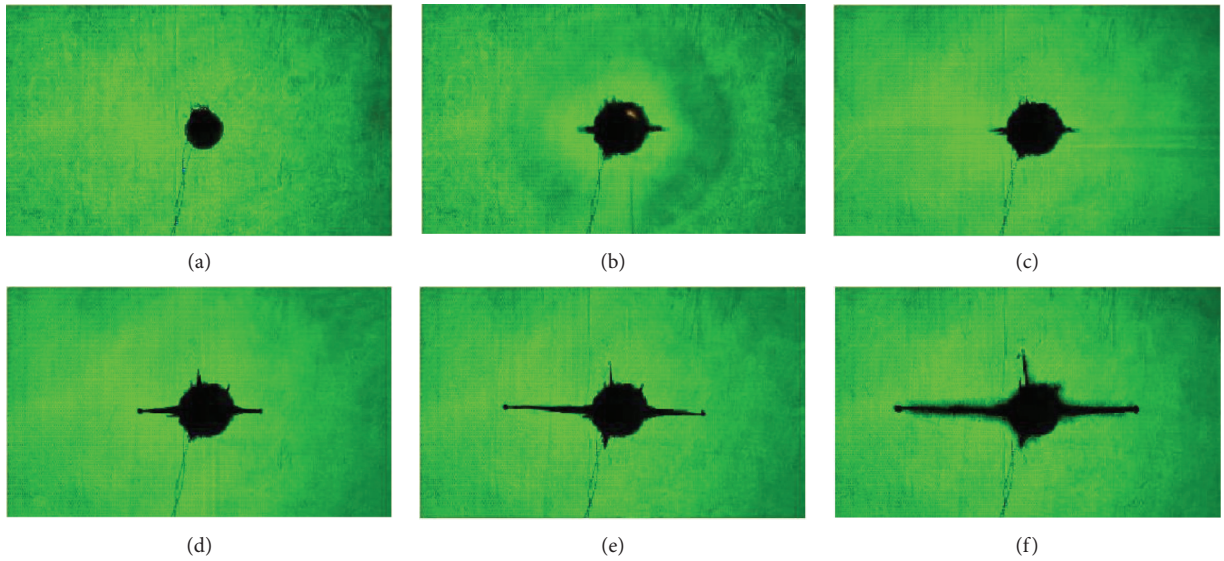

Figure 4: Test results of blasting crack of shaped charge [29]. (a) $t = 0\,\mu$s, (b) $t = 20\,\mu$s, (c) $t = 80\,\mu$s, (d) $t = 120\,\mu$s, (e) $t = 400\,\mu$s, (f) $t = 600\,\mu$s.

Table 1: Explosive and parameters of equation of state.

ρ (g·cm^{-3})	v_D (cm·μs^{-1})	A (GPa)	B (GPa)	R_1	R_2	ω	E (GPa)
1.3	0.4	214.4	0.182	4.2	0.9	0.15	4.192

Table 2: Mechanical parameter of PVC.

Material	Density (g·cm^{-3})	Elastic modulus (GPa)	Poisson's ratio (μ)
PVC	1.3	3.0	0.38

Table 3: Material parameters of the HJC model.

Parameters	Property	Value
ρ (g·cm^{-3})	Density	2.18
G (GPa)	Shear modulus	14.86
A	Normalized cohesive strength	0.79
B	Normalized pressure hardening	1.60
C	Strain rate coefficient	0.007
S_{fmax}	Normalized maximum strength	7
ε_{fmin}	Amount of plastic strain before fracture	0.01
N	Pressure hardening exponent	0.61
T (MPa)	Maximum tensile hydrostatic pressure	4
D_1	Damage constant 1	0.04
D_2	Damage constant 2	1
K_1 (GPa)	Pressure constant 1	85
K_2 (GPa)	Pressure constant 2	−171
K_3 (GPa)	Pressure constant 3	200

4. Analysis on Crack Evolution of Elliptical Bipolar Linear Shaped Charge Blasting

4.1. Geometric Model of Numerical Calculation. In order to analyze the dynamic evolution law of blasting cracks with different blast hole diameters, the quasi two-dimensional calculation models with various blast hole diameters of 42 mm, 50 mm, 60 mm, 70 mm, 80 mm, 90 mm, and 100 mm were established, respectively. The shaped charge is an elliptical bipolar linear structure, the energy gathering tube is made of PVC material, the thickness of the shell of the energy gathering tube is 2 mm, the thickness of the layer liner is 1.4 mm, and the angle of the shaped charge groove is 70°. The calculation model is shown in Figure 6, and no reflective boundary condition is set around the model.

Select a measuring point every 10 mm along the blast hole radial in the concentrating energy direction and the nonconcentrated energy direction. The concentrating energy direction is numbered as #G1 ~ #G5 from near to far, and the nonconcentrated energy direction is numbered as #N1 ~ #N5 from near to far. The layout of each measuring point is shown in Figure 7.

4.2. Analysis of Rock Crack Development with Blast Hole Diameter 42 mm

4.2.1. Analysis of Initial Crack Formation. After the shaped charge is detonated in the blast hole, the detonation wave acts on the shaped charge cover with huge pressure at 5 μs to form a high-temperature, high-pressure, high-energy shaped charge jet. The jet first acts on the blast hole wall and forms a guide crack on the rock in this direction, as shown in Figure 8. In other directions of the blast hole, the shell of the shaped charge has instantaneous buffering and inhibiting effect on the detonation products and the air medium between the shell of the shaped charge and the blast hole wall has a buffering effect, which greatly reduces the direct effect and damage degree of the shock wave on the blast hole wall, thus inhibiting the development of cracks.

4.2.2. Stress Time History Analysis. The stress time history curves of each measuring point are shown in Figures 9 and 10.

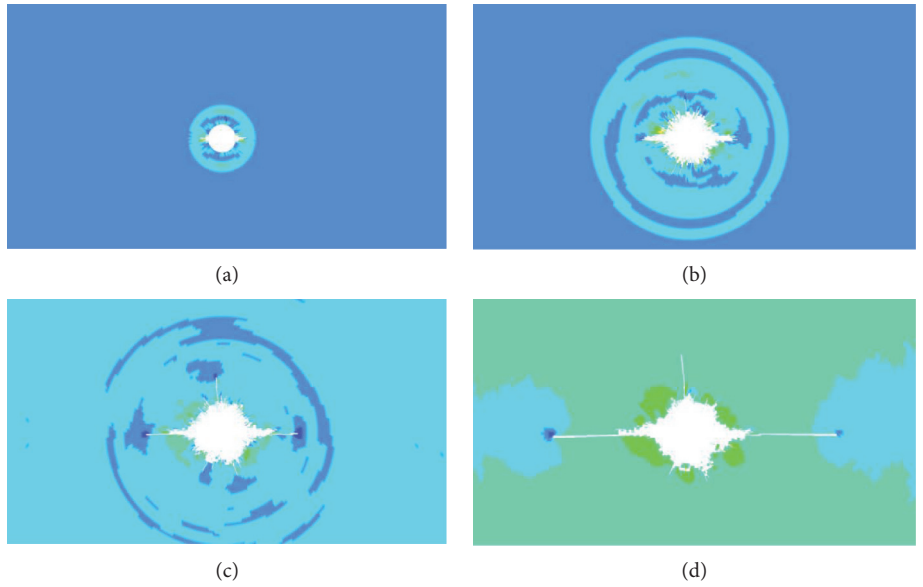

Figure 5: Numerical simulation results of blasting crack development of shaped charge. (a) $t = 20\,\mu s$, (b) $t = 80\,\mu s$, (c) $t = 120\,\mu s$, (d) $t = 600\,\mu s$.

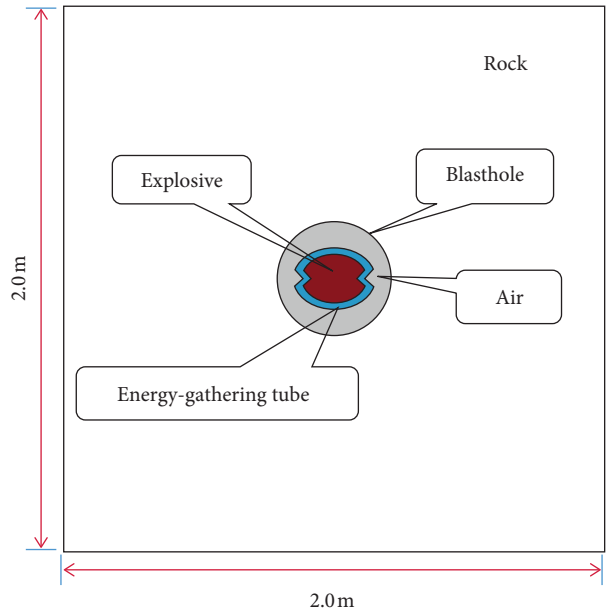

Figure 6: Schematic of the numerical calculation model.

The above curves suggested that the peak attenuation rate of rock equivalent stress is very fast along the center of the blast hole outward in both the concentrating energy and nonconcentrated energy directions. Especially, the maximum equivalent stress in the direction of shaped charge is 39.25 MPa, the maximum equivalent stress in the direction of nonshaped charge is 17.33 MPa, and the maximum effective stress in the direction of concentrating energy is about 2.3 times of that in the direction of nonconcentrated energy. The results indicated that the ability of rock penetration in the direction of concentrating energy is much greater than that in the direction of nonconcentrated energy.

4.2.3. Crack Propagation Analysis. After the initial guide crack is formed, the explosive detonation product fills the whole blasting cavity, and the quasi-static load is applied to the rock on the blast hole wall. Under the quasi-static load and stress concentration, the tip of the guide crack forms a long crack and propagates.

Figure 11 shows the crack development of 42 mm blast hole in elliptical bipolar linear shaped charge blasting. At $80\,\mu s$, microcracks begin to appear outside the direction of concentrating energy. At $120\,\mu s$, both main cracks and microcracks keep growing. At $300\,\mu s$, the cracks outside the direction of concentrating energy tend to stop growing. At

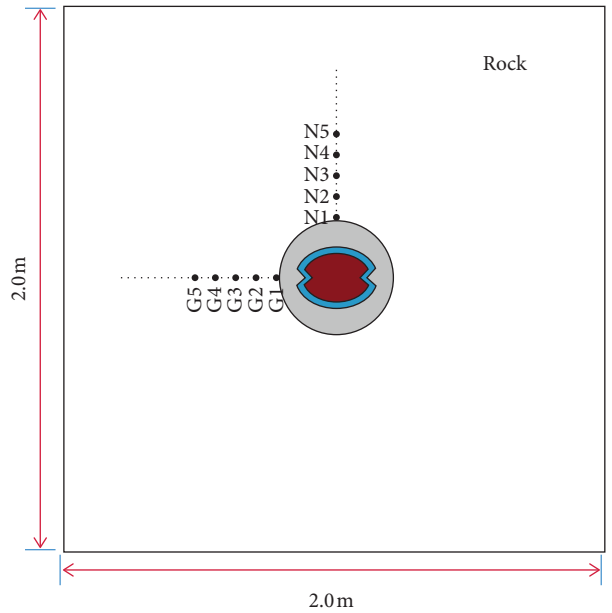

Figure 7: The layout of measuring points.

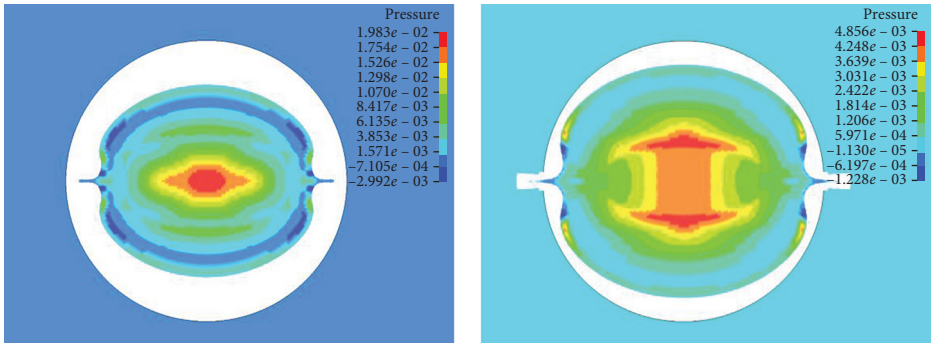

(a) (b)

Figure 8: Initial crack formation. (a) $t = 5\,\mu s$, (b) $t = 8\,\mu s$.

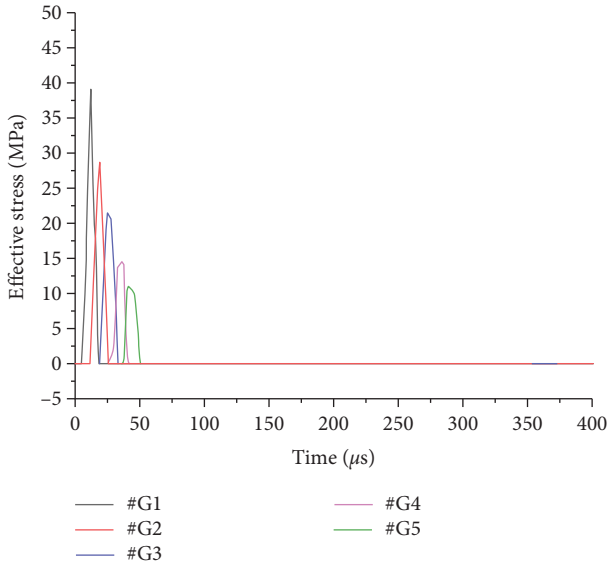

Figure 9: Effective stress time history curve in the concentrating energy direction.

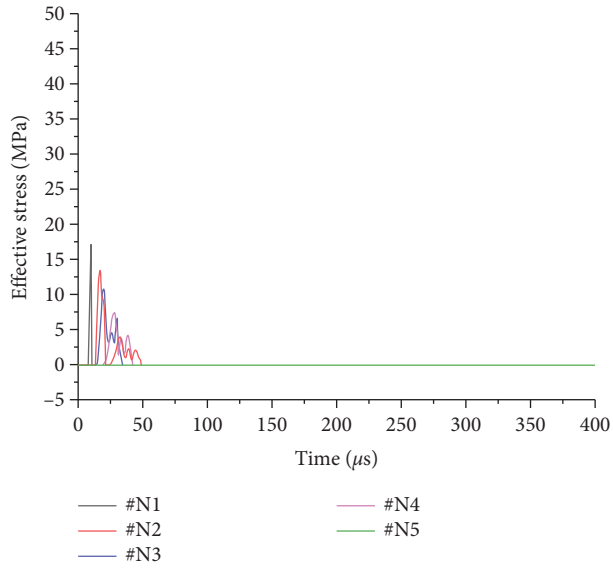

Figure 10: Effective stress time history curve in the nonconcentrated energy direction.

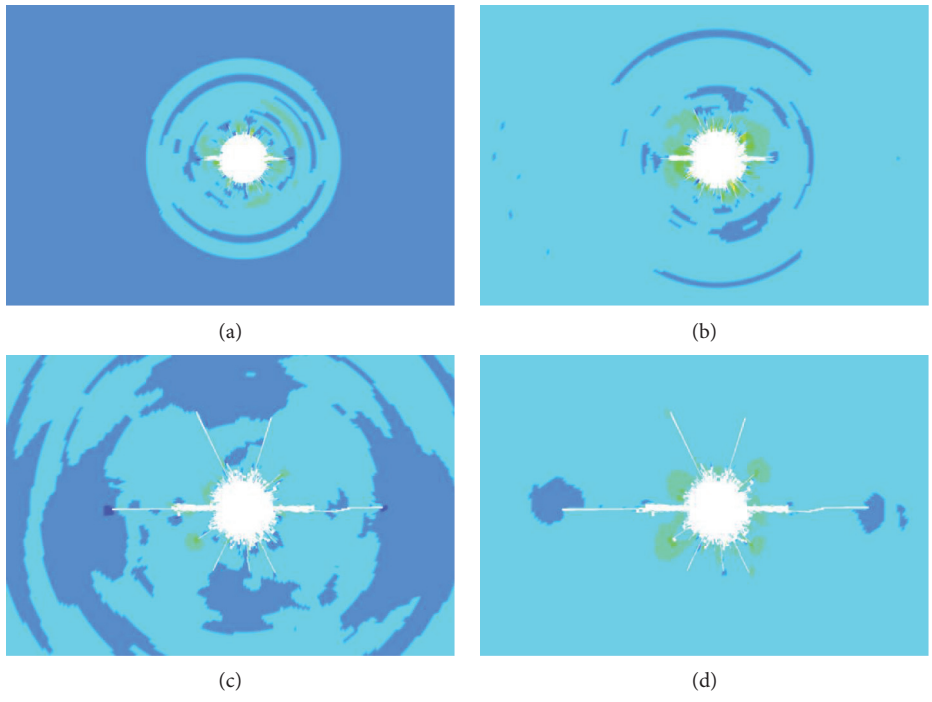

Figure 11: Crack development with blast hole diameter 42 mm. (a) $t = 80\,\mu s$, (b) $t = 120\,\mu s$. (c) $t = 300\,\mu s$, (d) $t = 600\,\mu s$.

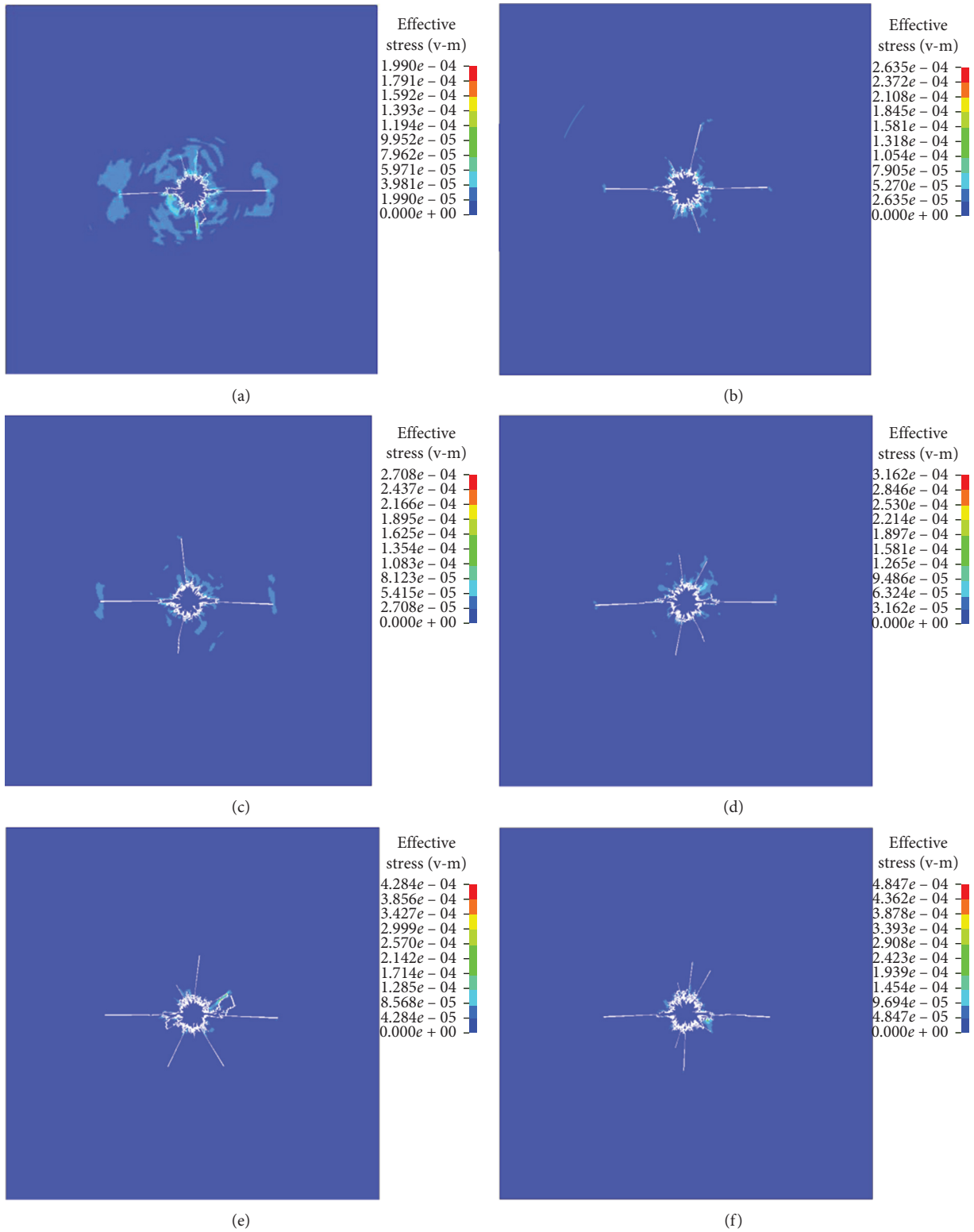

Figure 12: Crack development with different blast hole diameters. (a) $D = 50$ mm, (b) $D = 60$ mm, (c) $D = 70$ mm, (d) $D = 80$ mm, (e) $D = 90$ mm, (f) $D = 100$ mm.

Table 4: Main crack length of different hole diameter blasting.

Blast hole diameter	42 mm (cm)	50 mm (cm)	60 mm (cm)	70 mm (cm)	80 mm (cm)	90 mm (cm)	100 mm (cm)
Left main crack length	49.27	54.43	60.17	65.21	67.14	65.54	62.16
Right main crack length	49.27	57.40	62.16	65.32	67.44	65.64	63.16

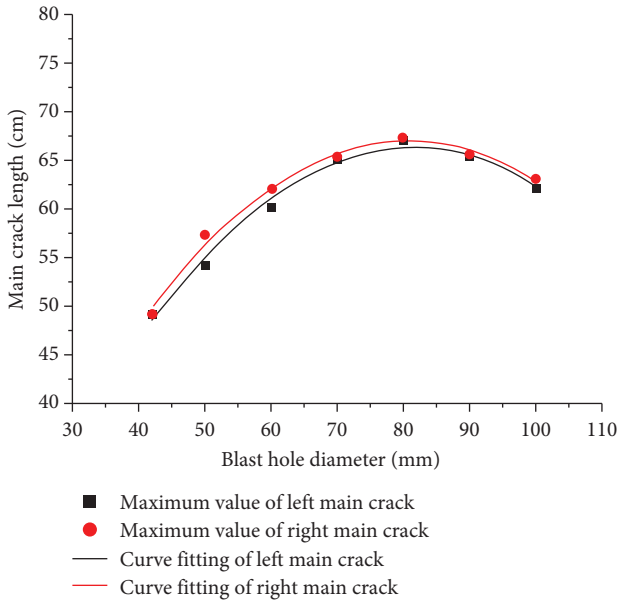

Figure 13: Relation curve between main crack length and blast hole diameter.

600 μs, all cracks tend to stop growing. The cracks in the direction of concentrating energy are always much larger than those in other directions.

4.3. Analysis of Rock Cracks Development with Different Blast Hole Diameter. Based on the established numerical model, the crack development of rock with various diameters of 50 mm, 60 mm, 70 mm, 80 mm, 90 mm, and 100 mm is analyzed. The results of crack development are shown in Figure 12.

The results in Figure 12 indicate that under the blasting of an elliptical bipolar linear shaped charge with different blast hole diameters, two main cracks are formed in the left and right concentrating energy direction, and random secondary cracks are also formed in other directions. With the increase in blast hole diameter, the length of the main crack first increases and then decreases, indicating that there is an optimal blast hole diameter.

4.4. Analysis of Radial Decoupling Coefficient. The radial decoupling coefficient changes with the change of blast hole diameter. The main crack length of different blast hole diameter blasting is shown in Table 4.

The curve fitting between the length of the main crack and the diameter of the blast hole is shown in Figure 13. The correlation coefficients between the blast hole diameter and the length of the left and right main cracks have reached more than 0.98. The best blast hole diameter is 82 mm.

Moreover, the equivalent charge diameter of the elliptical bipolar linear shaped charge blasting is 24.4 mm based on the above established numerical simulation model, and thus the best radial decoupling coefficient calculated is 3.36.

5. Conclusions

(1) Under the elliptical bipolar linear shaped charge blasting, the damage ability of rock penetrating in the concentrating energy direction is much greater than that in the nonconcentrated energy direction. The maximum effective stress of rock closed to the position of shaped charge in the concentrating energy direction is about 2.3 times of that in the direction of nonconcentrated energy.

(2) Under the elliptical bipolar linear shaped charge blasting, the left and right main cracks can be formed in the concentrating energy direction with different hole diameters, and the random secondary cracks can be formed in other directions.

(3) There is a certain relationship between the length of the main crack and the diameter of the blast hole under elliptical bipolar linear shaped charge blasting. The curve fitting shows that the main crack is the longest when the diameter of the blast hole is 82 mm; that is, the best decoupling coefficient is 3.36.

Data Availability

The data supporting the results of this study can be obtained upon request to the corresponding author.

Conflicts of Interest

The authors declare that they have no conflicts of interest regarding the publication of this paper.

Acknowledgments

The authors would like to express the appreciation for the financial support from the National Natural Science Foundation of China (51678164 and 51478118), the Guangxi Natural Science Foundation Program (2018GXNSFDA138009), the Guangxi Science and Technology Plan Projects (AD18126011), and the GDHVPS (2019).

References

[1] M. S. Wang, "An overview of development of railways, tunnels and underground works in China," *Tunnel Construction*, vol. 30, no. 4, pp. 351–364, 2010.

[2] S. M. Tian, W. Wang, and J. F. Gong, "Development and prospect of railway tunnels in China(including statistics of railway tunnels in China by the end of 2020)," *Tunnel Construction*, vol. 41, no. 2, pp. 308–325, 2021.

[3] J. X. Wang, B. P. Zou, and L. S. Hu, "Advance and trend in smooth blasting technology for tunnel and underground engineering," *Chinese Journal of Underground Space and Engineering*, vol. 9, no. 4, pp. 800–807, 2013.

[4] S. H. Cho, Y. Nakamura, B. Mohanty, H. S. Yang, and K. Kaneko, "Numerical study of fracture plane control in laboratory-scale blasting," *Engineering Fracture Mechanics*, vol. 75, no. 13, pp. 3966–3984, 2008.

[5] R. S. Yang, Y. B. Wang, H. J. Xue et al., "Dynamic behavior analysis of perforated crack propagation in two-hole blasting,"

Procedia Earth and Planetary Science, vol. 5, pp. 254–261, 2012.

[6] L. Yang, R. Yang, G. Qu, and Y. Zhang, "Caustic study on blast-induced wing crack behaviors in dynamic-static superimposed stress field," *International Journal of Mining Science and Technology*, vol. 24, no. 4, pp. 417–423, 2014.

[7] R. Yang, Y. Wang, and C. Ding, "Laboratory study of wave propagation due to explosion in a jointed medium," *International Journal of Rock Mechanics and Mining Sciences*, vol. 81, pp. 70–78, 2016.

[8] R. S. Yang, Y. B. Wang, D. M. Guo et al., "Experimental research of crack propagation in polymethyl methacrylate material containing flaws under explosive stress waves," *Journal of Testing and Evaluation*, vol. 44, no. 1, pp. 56–60, 2016.

[9] Z. W. Yue, L. Y. Yang, and Y. B. Wang, "Experimental study of crack propagation in polymethyl methacrylate material with double holes under the directional controlled blasting," *Fatigue and Fracture of Engineering Materials and Structures*, vol. 36, no. 8, pp. 827–833, 2013.

[10] Z. W. Yue, S. C. Zhang, P. Qiu et al., "Influence of charge structures on the slotted cartridge blasting effect," *Journal of Vibration and Shock*, vol. 37, no. 10, pp. 27–34, 2018.

[11] Z. W. Yue, S. Y. Tian, S. C. Zhang et al., "Expanding law of cracks formed by slotted cartridge blast under unidirectional confining pressure," *Journal of Vibration and Shock*, vol. 38, no. 23, pp. 186–195, 2019.

[12] Z. W. Yue, X. B. Hu, Z. Y. Chen et al., "Experimental study of effect of uncoupled charge on energy utilization efficiency of explosives," *Blasting*, vol. 37, no. 3, pp. 34–39, 2020.

[13] Y. Wang, "Study of the dynamic fracture effect using slotted cartridge decoupling charge blasting," *International Journal of Rock Mechanics and Mining Sciences*, vol. 96, pp. 34–46, 2017.

[14] Y. Luo, "Study on application of shaped charge in controlled rock mass blasting technology," *Journal of Disaster Prevention and Mitigation Engineering*, vol. 27, no. 1, pp. 57–62, 2001.

[15] Y. Luo, Z. W. Sheng, and X. R. Cui, "Application study on blasting with linear cumulative cutting charge in rock," *Chinese Journal of Energetic Materials*, vol. 3, no. 14, pp. 236–241, 2006.

[16] J. F. Qin, R. X. Qin, and B. H. Li, "Study and application of elliptical bipolar linear shaped charge," *Engineering Blasting*, vol. 15, no. 3, pp. 70–74, 2009.

[17] B. H. Li, W. F. Cui, S. L. Li et al., "Experimental investigation and numerical simulation of decouple coefficient of elliptic bipolar linear shaped charge," *Blasting*, vol. 30, no. 2, pp. 54–58, 2013.

[18] B. H. Li, *Research on Theory and Application Technology of Elliptic Bipolar Linear Shaped Charge's Presplit blasting*, Central South University, Changsha, China, 2013.

[19] B. Wu, H. Wei, S. Xu et al., "Analysis of the cracking mechanism of an elliptical bipolar linear-shaped charge blasting," *Advances in Civil Engineering*, vol. 2021, Article ID 6669704, 12 pages, 2021.

[20] B. Wu, H. Wei, S. Xu et al., "Numerical study of two-way shaped charge blasting with different charge structures," *Engineering Blasting*, vol. 27, no. 1, pp. 14–21, 2021.

[21] B. Wu, H. Wei, S. Xu et al., "Research on numerical optimization of smooth blasting layer parameters of shaped energy smooth blasting," *Nonferrous Metals Engineering*, vol. 10, no. 12, pp. 113–121, 2020.

[22] B. W. Xia, C. W. Liu, Y. Y. Lu et al., "Experimental study of propagation of directional fracture with slotting hydraulic blasting," *Journal of China Coal Society*, vol. 41, no. 2, pp. 432–438, 2016.

[23] D. Y. Guo, H. B. Pei, J. C. Song et al., "Study on splitting mechanism of coal bed deep-hole cumulative blasting to improve permeability," *Journal of China Coal Society*, vol. 33, no. 12, pp. 1381–1385, 2008.

[24] M. C. He, W. F. Cao, R. L. Shan et al., "New blasting technology-bilateral cumulative tensile explosion," *Chinese Journal of Rock Mechanics and Engineering*, vol. 22, no. 12, pp. 2047–2051, 2003.

[25] D. Y. Guo, D. Y. Shang, P. F. Lu et al., "Experimental research of deep-hole cumulative blasting in hard roof weakening," *Journal of China Coal Society*, vol. 38, no. 7, pp. 1149–1153, 2013.

[26] Q. Li, Y. Liang, K. K. Ren et al., "Experimental study of propagation of directional cracks with shaped charge under blasting load," *Chinese Journal of Rock Mechanics and Engineering*, vol. 29, no. 8, pp. 1684–1689, 2010.

[27] N. Murphy, M. Ali, and A. Ivankovic, "Dynamic crack bifurcation in PMMA," *Engineering Fracture Mechanics*, vol. 73, no. 16, pp. 2569–2587, 2006.

[28] H. P. Rossmanith, A. Daehnke, R. E. K. Nasmillner, N. Kouzniak, M. Ohtsu, and K. Uenishi, "Fracture mechanics applications to drilling and blasting," *Fatigue and Fracture of Engineering Materials and Structures*, vol. 20, no. 11, pp. 1617–1636, 1997.

[29] Y. L. Che, *Study on the Mechanism of Irregular Cartridge and the Damage of Surrounding Rock*, China University of Mining and Technology, Xuzhou, China, 2015.